Dynamics of Sept4 expression in fibrotic livers of mice infected with *Schistosoma japonicum*

Y. N. DUAN*†, H. Y. QIAN†, Y. W. QIN, D. D. ZHU, X. X. HE, Q. ZHOU, Y. N. YANG, J. BAO, J. R. FENG, W. SUN *and* J. L. CHEN

Department of Parasitology and Microbiology, School of Medicine, Nantong University; Nantong, Jiangsu Province, 226001, People's Republic of China

(*Received 7 January 2011; revised 25 January 2011; accepted 28 March 2011; first published online 17 June 2011*)

SUMMARY

In order to investigate the dynamics of Septin4 (Sept4) expression and its function in the formation of fibrotic livers in mice infected with *Schistosoma japonicum*, we constructed the mouse model of *S. japonicum* egg-induced liver fibrosis for 24 weeks. Immunohistochemical staining, qRT-PCR and Western blot were used to detect the expression of Sept4 and α-smooth muscle actin (α-SMA). We found Sept4 localized in the perisinusoidal space where hepatic stellate cells (HSCs) distribute in the periphery of circumoval granulomas and the portal venule. The expression of Sept4 and α-SMA had a similar significant tendency of an up-regulation to a peak at 12 weeks post-infection (p.i.) followed by a down-regulation. At 24 weeks p.i. both were at a low level. These results suggest that Sept4 and α-SMA may interact together in HSCs. Based on this evidence, we hypothesize that Sept4 seems to be involved in the formation of inflammatory granulomata and subsequent liver fibrosis by regulating HSCs activation.

Key words: Septin4, hepatic stellate cells, *Schistosoma japonicum*, liver fibrosis.

INTRODUCTION

Schistosomiasis is a chronic parasitic disease that affects more than 200 million people in 74 countries worldwide, mostly in developing countries, causing approximately 20 000 deaths per year (Zhang *et al*. 2001). The reason for the severe mortality is that *S. japonicum* eggs can induce liver fibrosis and progress to portal blood hypertension, varicose veins and ascites (Arnaud *et al*. 2008). After schistosome infection, adult worms locate to the tributaries of the portal vasculature. Females continuously release eggs that pass into the intestine. The portal blood flow, however, carries some eggs to the liver where they are lodged in small vessels of the portal tracts to induce delayed-type hypersensitivity reactions against the eggs, which leads to the formation of inflammatory granulomata and subsequent liver fibrosis (Friedman, 2003).

Liver fibrosis is a wound-healing response, characterized by excessive deposition of extracellular matrix (ECM) proteins that disrupt the normal architecture of the liver. In this process, HSCs which reside in the Disse's space outside the liver sinusoids, maintain a quiescent phenotype and store vitamin A under physiological conditions, play a crucial role (Friedman, 2000; Bataller and Brenner, 2001). HSCs are activated and become myofibroblastic cells that express α-SMA as a representative marker (Friedman, 2000; Carpino *et al*. 2005). In addition, HSCs posses the activation characterized by proliferation, contraction, migration, secretion of several pro-fibrogenic mediators and generation of extracellular matrix materials such as types I and III collagen (Friedman, 2008). All these events result in an intense periportal fibrosis and progressive occlusion of the portal veins, which leads to the development of portal hypertension, splenomegaly, ascites, portocaval shunting, gastrointestinal varices and bleeding that may eventually be fatal (Burke *et al*. 2009).

The Septins are a family of polymerizing GTP-binding proteins originally discovered in budding yeast as a group of cell-cycle mutants which cause defects in cytokinesis (Field and Kellogg, 1999). In mammals, Septins are involved in cytoskeletal organization in mitosis, exocytosis and other cellular processes (Kinoshita, 2006). Previous reports showed expression of Sept4 mRNA in the liver (Zieger *et al*. 2000; Ihara *et al*. 2005) and alteration of the level of Sept4 mRNA in HSCs during fibrotic change *in vivo* and *in vitro* (De Minicis *et al*. 2007). Recently, a report showed that the HSC-specific Septin subunit Sept4 is involved in the suppressive modulation of myofibroblastic transformation and liver fibrogenesis with the model of carbon tetrachloride (CCl4) and bile duct ligation (BDL) treatment (Iwaisako *et al*. 2008). It is known that CCl4 as a chemical and BDL as a physical injury can induce liver fibrosis, However, *S. japonicum*-induced egg granuloma and subsequent liver fibrosis is a complex immunopathogenic process. It is immunologically characterized by

* Corresponding author: Tel: +86 513 85051738. E-mail: yinongduan@Gmail.com
† These authors contributed equally to this work.

Parasitology (2011), **138**, 1003–1010.
doi:10.1017/S0031182011000667

switching from an early Th1 response to a Th2-dominated response after the onset of parasite egg production (Wilson *et al*. 2007). Then the egg can induce a granulomatous response in the liver which may eventually cause extensive tissue fibrosis (Wynn *et al*. 2004). Since the inducements are varied, the Sept4 expression pattern in the mouse model of *S. japonicum* egg-induced liver fibrosis remains unknown. The question therefore remains as to whether the Sept4 expression pattern will change or remain accordant?

In this study, we investigated the dynamics of Sept4 expression and the network of α-SMA filaments and Sept4 in mouse fibrotic liver induced by *S. japonicum*.

MATERIALS AND METHODS

Animals and parasites

Sixty-two male ICR mice, weighing 18–22 g, were purchased from the Center for Experimental Animals of Nantong University. Mice were housed under a 12 h light cycle, and fed with pathogen-free food and water. *Schistosoma japonicum* cercariae released from infected intermediate host snail *Oncomelania hupensis* were provided by the Institute of Schistosomiasis Control (Jiangsu, China). Animal care and experimental procedures were approved by the Animal Ethics Committee of Nantong University.

Experimental infection

Fifty-six mice were taken randomly as the experimental group, and each mouse was infected with 20–25 *S. japonicum* cercariae via shaved abdominal skin. The other 6 mice were taken as the normal control group and were not infected. After the control group mice were sacrificed, liver tissues from 3 mice were fixed by 4% paraformaldehyde/PBS and the remaining tissues were kept in liquid nitrogen. In order to observe the development of liver fibrosis, 6 mice from the experimental group were sacrificed randomly at fortnightly intervals from 4 to 12 weeks p.i. and at 4-week intervals from 12 to 24 weeks p.i. Livers were kept in the same way.

Sirius red staining

The mice livers, after portal perfusion, were fixed with 4% paraformaldehyde/PBS, frozen, and cryosections were cut at 5 μm thickness. The specimens were incubated for 1 h at room temperature with an aqueous saturated solution of picric acid containing 0·1% Sirius red (Sigma F3B). Images of 6 random microscopic fields of red-stained collagen fibres in the liver section of each mouse were recorded using an erected microscope and then digitized and analysed on Image-Pro Plus software. Experiments were repeated thrice to ensure reproducible results.

Reverse transcription-coupled, quantitative polymerase chain reaction (qRT-PCR)

Samples of 100 mg live from each mouse were homogenized in 1 ml of Trizol (Sigma-Aldrich, USA) in a tissue grinder and the total RNA was isolated as recommended by the manufacturer. Reverse-transcribed used RevertAid™ First Strand cDNA Synthesis Kits (MBI Fermentas, K1622#, Canada) with random hexamers. For quantitative real-time PCR, we followed the SYBR® Premix Ex Taq™ RT-PCR Kit (DRR041A, TaKaRa) and used the following primers: mouse Sept4 sense 5′-TGAAGGAACGGAATCGCAAC-3′ and antisense 5′-CTGGCATAGGCAGGAAAAGAG-3′ (NM_011129); mouse α-SMA sense 5′-CGCGACATCAAAGAGAA GC-3′ and antisense 5′-ATCCCCGCAGACTCCATAC-3′ (X13297); mouse collagen, type I, alpha1 (Collagen α1 (I)) 5′-GCCCGGAAGAATACG-3′ and antisense 5′-ACATCTGGGAAGCAAA-3′ (NM_007742). As an internal control, we amplified mouse GAPDH with the following primer set: sense 5′-GGTGAAGGTCGGTGAACG-3′ and antisense 5′-CTCGCTCCTGGAAGATGGTG-3′. Experiments were completed on Rotor-Gene (Corbett Research, RG-3000, Australia) and were repeated thrice using samples obtained from different mice to ensure reproducible results. Rotor-Gene 3000 Series software and SigmaPlot 10.0 were used to analyse the results.

Immunofluorescence

For immunofluorescence, frozen liver was sectioned at a thickness of 5 μm, fixed on microscope slides with 4% paraformaldehyde/PBS, permeabilized with 1% TritonX-100, and labelled with antibodies for Sept4 (rabbit polyclonal, sc-20179, Santa Cruz, 1:200 dilutions) and desmin (goat polyclonal, sc-7559, Santa Cruz, 1:200 dilutions), then with fluorescein isothiocyanate-conjugated (705-095-003, Jackson ImmunoResearch, 1:100 dilutions) or rhodamine-conjugated (111-025-003, Jackson ImmunoResearch, 1:800 dilutions) secondary antibodies. The coverslips were examined in a Leica confocal microscope. Digitized images of the fluorescent antibody-stained sections were acquired with software provided by Leica.

Immunohistochemistry

The liver was fixed with 4% paraformaldehyde/PBS, frozen, and cryosectioned at a thickness of 5 μm. For immunohistochemistry, the sections were treated by antigen retrieval with autoclave heating (pH 6·0

https://doi.org/10.1017/S0031182011000667 Published online by Cambridge University Press

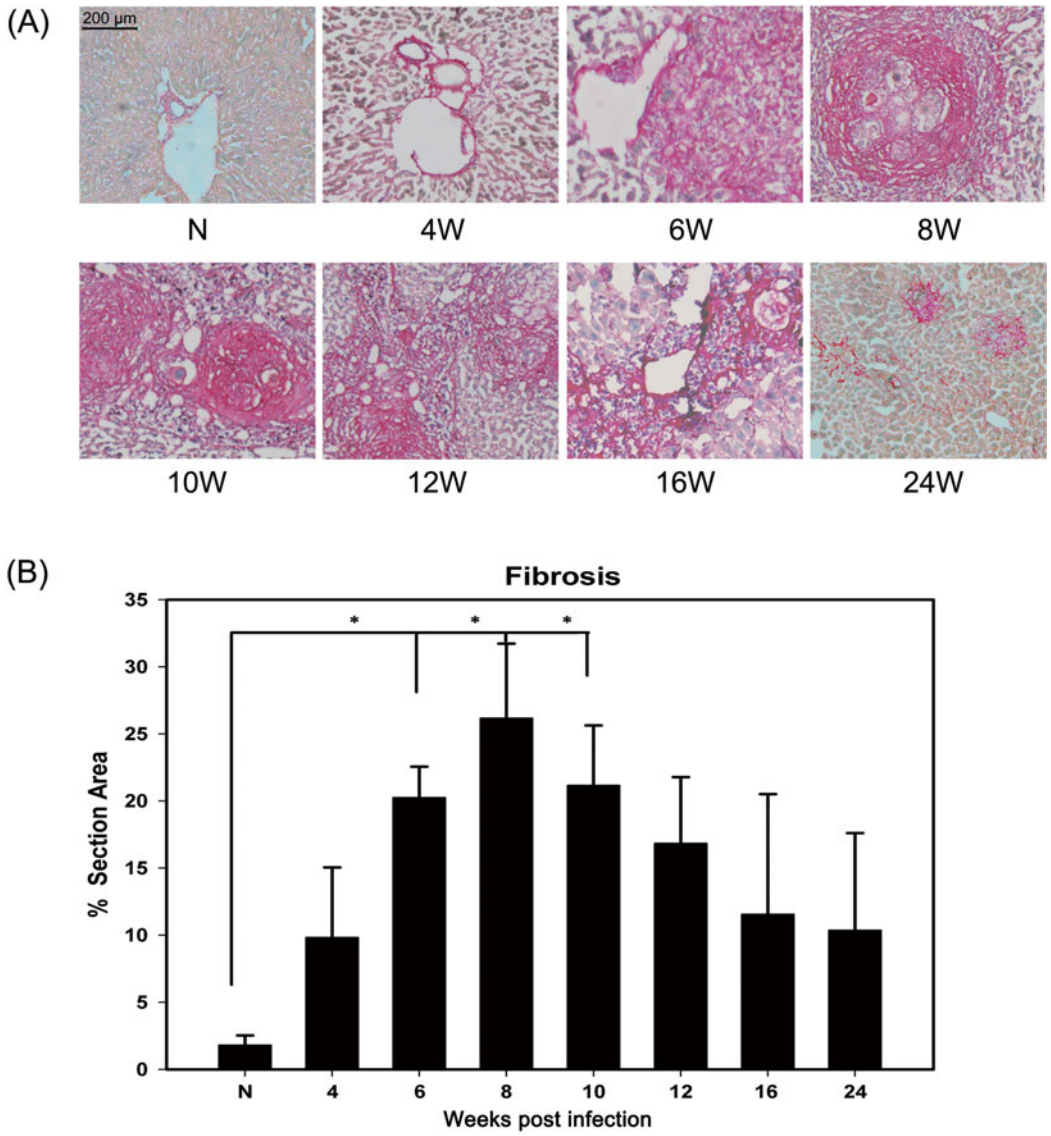

Fig. 1. Images of liver slices stained with Sirius red (×100 magnification) over the course of *Schistosoma japonicum* infection in mice. (A) Sirius red staining of the sections. At the early stage, collagen deposition was mainly at the periphery of egg granulomas and then it extended into the surrounding hepatic parenchyma. (B) Quantification of the collagen staining area. After 4 weeks p.i., collagen deposition became striking and at 8 weeks p.i. peaked. Values are means ± S.E.M. (* $P < 0{\cdot}05$, *vs* N). Experiments were repeated thrice from different mice.

citrate buffer), at 121 °C for 20 min. The sections were incubated with primary antibodies: α-SMA (rabbit polyclonal, ab5694, abcam, 1:400 dilutions), Sept4 and secondary antibodies (HRP-conjugated goat anti-rabbit IgG, icllab, 1:200 dilutions), and the colour reaction was developed in 3-3′-diaminobenzidine and sections were counterstained with 10% Mayer's haematoxylin. Negative controls consisted of omission of the primary antibody, and replacement by non-immune serum. Digitized images of the sections were acquired with software provided by Leica.

Western blot

Tissue was homogenized and sonicated in buffer A (10 mM Tris–HCl, pH 7·6, containing 0·15 M NaCl, 1% Triton X-100, 0·1% sodium dodecyl sulfate, 0·1% sodium deoxycholate and protease inhibitors). The homogenate was centrifuged at 15 000 ***g*** at 4 °C for 0·5 h, and the protein concentration in the supernatant was quantified by the Bradford method. The protein solution was heat-denatured with an equal volume of 2 × SDS Laemmli sample buffer for 10 min. Proteins were loaded into wells of a 10% (w/v) acryl/*bis*acrylamide gel and, after separation, proteins were transferred to a polyvinylidene fluoride (PVDF) membrane. After saturation in Tris-buffered saline Tween-20 (TBST) containing 5% milk, the primary antibody (Sept4 for 1:200 dilutions; α-SMA for 1:200 dilutions) and the secondary antibody diluted in TBST (HRP-conjugated goat anti-rabbit IgG, icllab, 1:800 dilutions) were sequentially added to and incubated with the membranes for overnight and 2 h, respectively. Reaction was obtained by enhanced

https://doi.org/10.1017/S0031182011000667 Published online by Cambridge University Press

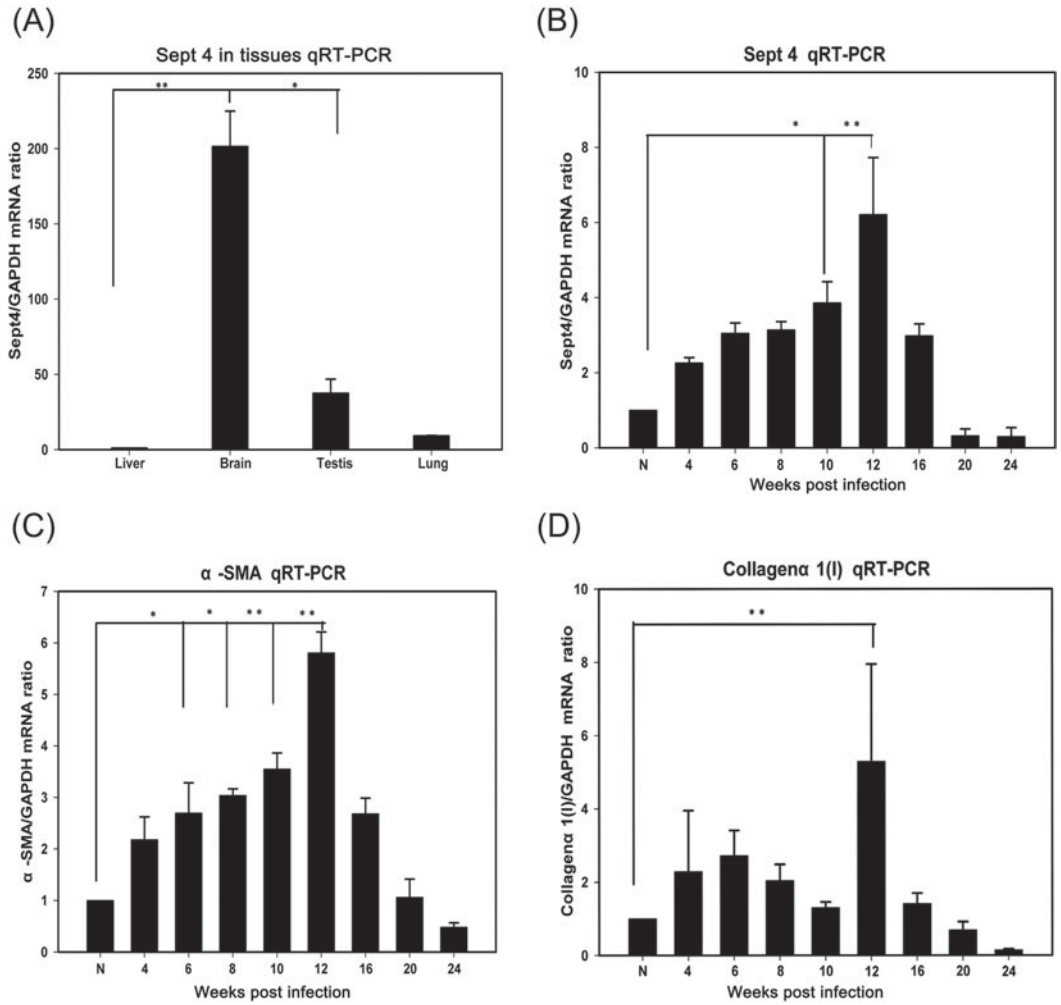

Fig. 2. Gene expression of Sept4, α-SMA, collagen α1 (I) in mice liver over the course of *Schistosoma japonicum* infection by qRT-PCR. (A) Detection of Sept4 expression in different tissues of normal mice by qRT-PCR. Expression of Sept4 is higher in brain and testis than that in liver. (B-C) Both Sept4 and α-SMA were remarkably up-regulated to peak at 12 weeks p.i. A significant reduction was observed subsequently. (D) Collagen α1 (I) expression appeared as a small peak at 6 weeks p.i. and a large peak at 12 weeks p.i. following a major descent. Values are means ± S.E.M. (*$P<0{\cdot}05$; **$P<0{\cdot}01$ *vs* N). Experiments were repeated thrice from different mice.

chemiluminescence (ECL). Each Western blot was repeated thrice using samples obtained from different mice to ensure reproducible results.

Quantification and statistics

All data were expressed as means ± S.E.M. of at least 3 experiments. Data were compared using the Student's t-test. P values less than 0·05 were considered statistically significant.

RESULTS

Sirius red staining for collagen (Fig. 1) was carried out to estimate fibrosis reactivity. From 6 to 10 weeks p.i., collagen was distributed mainly at the periphery of egg granulomas and then extended into the surrounding hepatic parenchyma. The collagen-positive area covered only about 1·8% of the liver section at 4 weeks p.i. but was up-regulated significantly to more than 25% at 8 weeks p.i. to reach a peak ($P<0{\cdot}05$). This result was in accordance with published reports (Bartley *et al*. 2006), suggesting that our mouse model of *S. japonicum* egg-induced liver fibrosis was constructed successfully.

qRT-PCR analysis of normal mouse tissues (Fig. 2) showed the highest Sept4 expression in brain, a lesser extent in testis and lung and the lowest in liver, normalized with GAPDH which was accordant to the previous reports findings (Kinoshita *et al*. 2000; Kissel *et al*. 2005). Sept4 expression at the mRNA level was low in normal mice liver, but in fibrotic mice, Sept4 expression, normalized with GAPDH, was remarkably up-regulated to about 3·9 at 10 weeks p.i. (*vs* N, $P<0{\cdot}05$) and 6·2 at 12 weeks p.i. (*vs* N, $P<0{\cdot}01$). A significant reduction was observed subsequently and the ratio of Sept4/GAPDH reached 0·3 at 24 weeks p.i. Gene transcription of α-SMA and collagen α1 (I), which is associated with HSC activation and the deposition of

https://doi.org/10.1017/S0031182011000667 Published online by Cambridge University Press

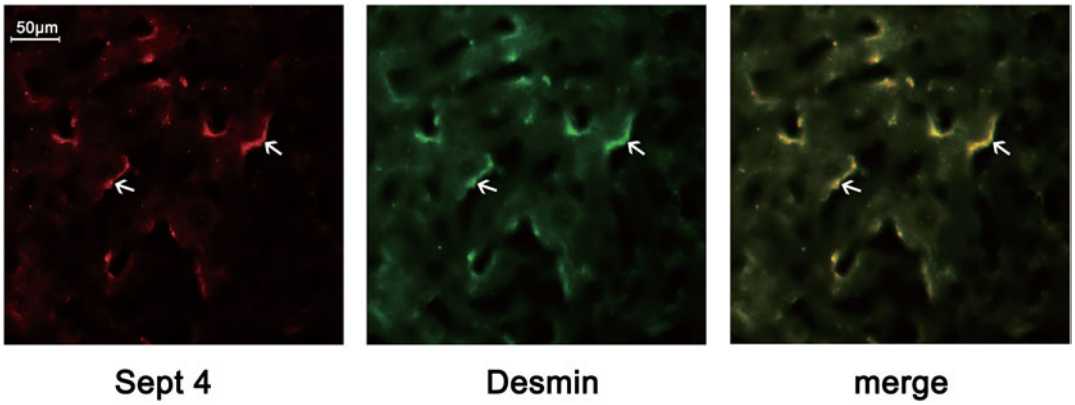

Fig. 3. Double immunolabelling analyses of the Sept4 and desmin in liver sections 10 weeks p.i. Sept4 and desmin were labelled respectively with fluorescein TRITC (red) and FITC (green) (magnification ×400). Both the green signal for desmin and red signal for Sept4 were co-localized in the peri-sinusoidal space as the white arrows pointed where HSCs exist.

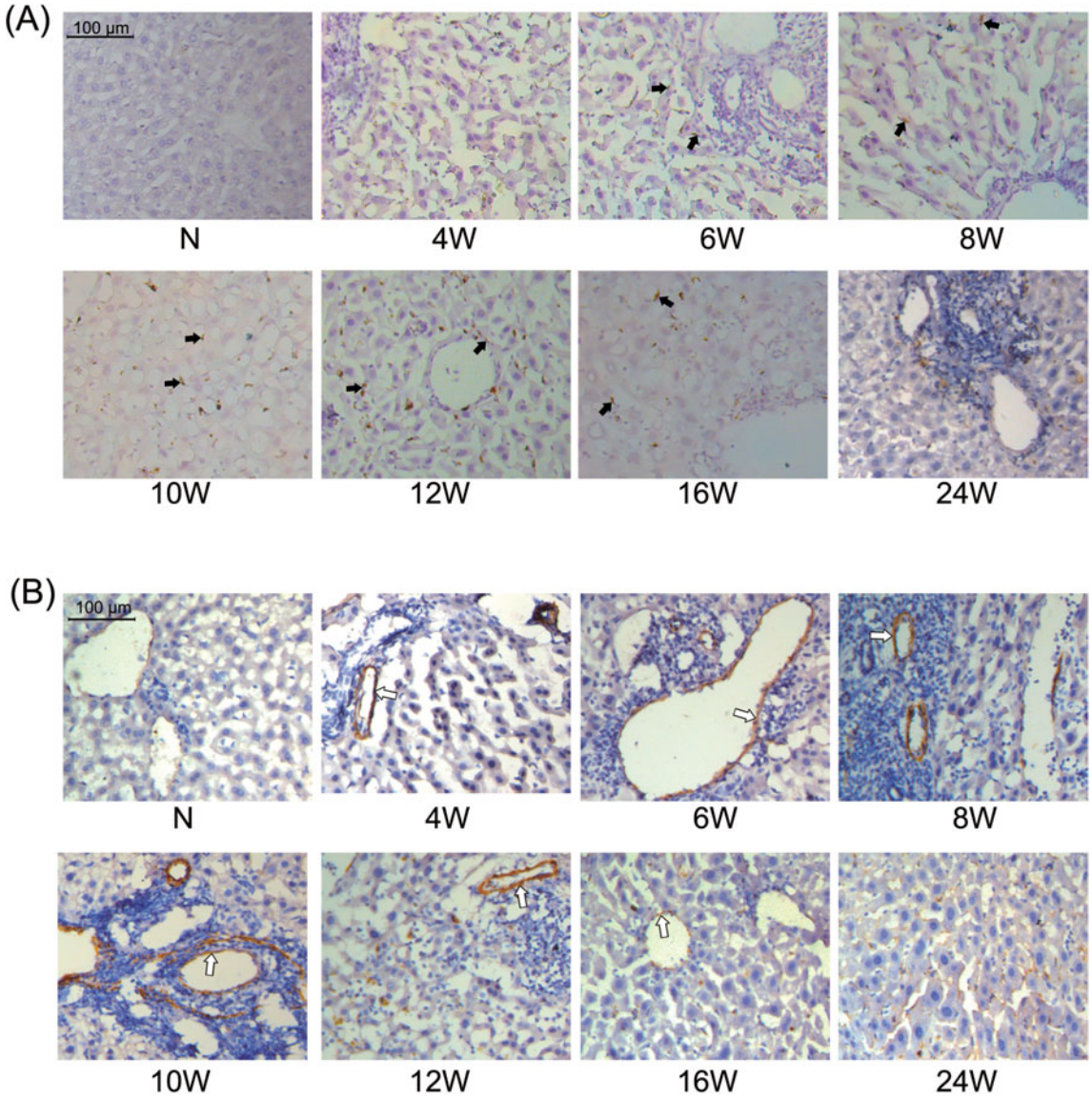

Fig. 4. Representative micrographs showing the expression of Sept4 and α-SMA at each time-point (magnification × 200). (A and B) Immunohistochemical analysis of Sept4 and α-SMA. The black arrows point to the place where Sept4 is expressed (brown). The white arrows point to the place where α-SMA is expressed (brown). Both Sept4 and α-SMA were not present in the N group but were expressed strongly from 8 to 12 weeks p.i. in the peri-sinusoidal space of Disse at the periphery of egg granulomas and portal venule.

https://doi.org/10.1017/S0031182011000667 Published online by Cambridge University Press

fibrosis, respectively, was then detected. Interestingly, it was observed that the α-SMA/GAPDH ratio peaked at 5·8 at 12 weeks p.i. (*vs* N, $P<0·01$) and was then down-regulated to 0·48 at 24 weeks p.i. Therefore, the expression tendency of Sept4 and α-SMA at mRNA level was similar in the liver of mice infected with *S. japonicum*. Collagen α1 (I) expression appeared as a small peak at 6 weeks p.i., a larger peak at 12 weeks p.i. (*vs* N, $P<0·01$) followed by a dramatic reduction, as reported previously (Chen *et al*. 2002).

Double-labelling immunofluorescence was carried out with sections of liver at 10 weeks p.i. (Fig. 3). It is known that desmin is another characteristic marker of HSCs (Chang *et al*. 2009). Both the green signal for desmin and red signal for Sept4 were co-localized in the peri-sinusoidal space, which confirmed that Sept4 existed in peri-sinusoidal HSCs.

Immunohistochemical analysis of Sept4 and α-SMA (Fig. 4) demonstrated that neither of them were present in normal liver, although at the mRNA level they were detected. This might have been be due to the low expression of Sept4 and α-SMA. Sept4 was rare in the 4 weeks p.i. group but was visible in a time-dependent manner. Sept4 was distributed mainly at the periphery of egg granulomas from 6 to 8 weeks p.i. at the acute infection stage and then extended into the surrounding hepatic parenchyma especially near the portal venule at the chronic infection stage. α-SMA had a similar distribution.

Quantification of the immunohistochemical staining (Fig. 5) showed that Sept4-positive cells peaked at 12% of section area at 12 weeks p.i. (*vs* 4 weeks p.i., $P<0·01$) and was down-regulated to less than 2% at 24 weeks p.i. The area of α-SMA-positive cells extended to about 30% corresponding to the peak at 12 weeks p.i. (*vs* 4 weeks p.i., $P<0·01$) with subsequent reduction. In liver fibrosis, α-SMA is one of the accepted indicators of activated HSCs (Lindert *et al*. 2005). Taken together, our data suggested that Sept4 and α-SMA co-localized in HSCs at the periphery of egg granulomas and portal venules.

Western blot analysis (Fig. 6) demonstrated that Sept4, with a molecular weight of 55 kDa, was not detected in the livers from the normal group. A slight increase was seen as early as 4 weeks p.i., with a marked increase by 8 weeks p.i., and a continued increase to 12 weeks p.i. α-SMA, of molecular weight 42 kDa, was present in livers from the normal group at a low level. The relative level of Sept4 and α-SMA was evaluated by densitometric normalization against GAPDH. The ratios of Sept4 and α-SMA were, respectively, approximately 50% and 85% at the peak at 12 weeks p.i. followed by down-regulation (*vs* 4 weeks p.i., $P<0·01$) .

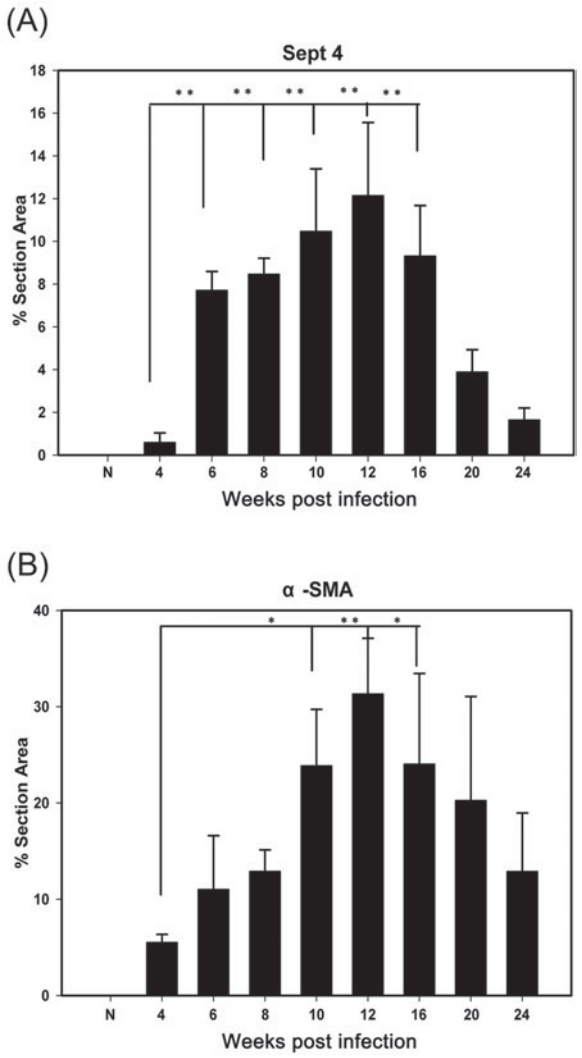

Fig. 5. Quantification of Sept4 and α-SMA immunohistochemical staining. (A and B) Sept4-positive cells covered 12% of the section area at 12 weeks p.i. and was down-regulated to less than 2% at 24 weeks p.i. α-SMA took about 30%, peaking at 12 weeks p.i., subsequently decreasing. However, α-SMA still retained about 12% at 24 weeks p.i. Values are means ± S.E.M. (*$P<0·05$; *$P<0·01$ *vs* 4 weeks p.i.). Experiments were repeated thrice from different mice.

DISCUSSION

In the present study, we investigated the dynamic changes of Sept4 expression in fibrotic livers of mice infected with *S. japonicum*. Our results revealed that Sept4 expression was up-regulated during the acute infection stage but was down-regulated during the chronic infection stage. The same tendency was observed also for α-SMA at both mRNA and protein levels in the mouse model of *S. japonicum* egg-induced liver fibrosis.

The finding that the expression of Sept4 at the mRNA level was low in normal liver, prompted us to assess whether *S. japonicum* egg-induced fibrotic liver could affect the expression of Sept4. We observed the dynamic changes of Sept4 expression by qRT-PCR, which demonstrated that its expression was highly up-regulated with the peak at the time-point of 12 weeks p.i. followed by down-regulation. This finding was consistent with previous research

https://doi.org/10.1017/S0031182011000667 Published online by Cambridge University Press

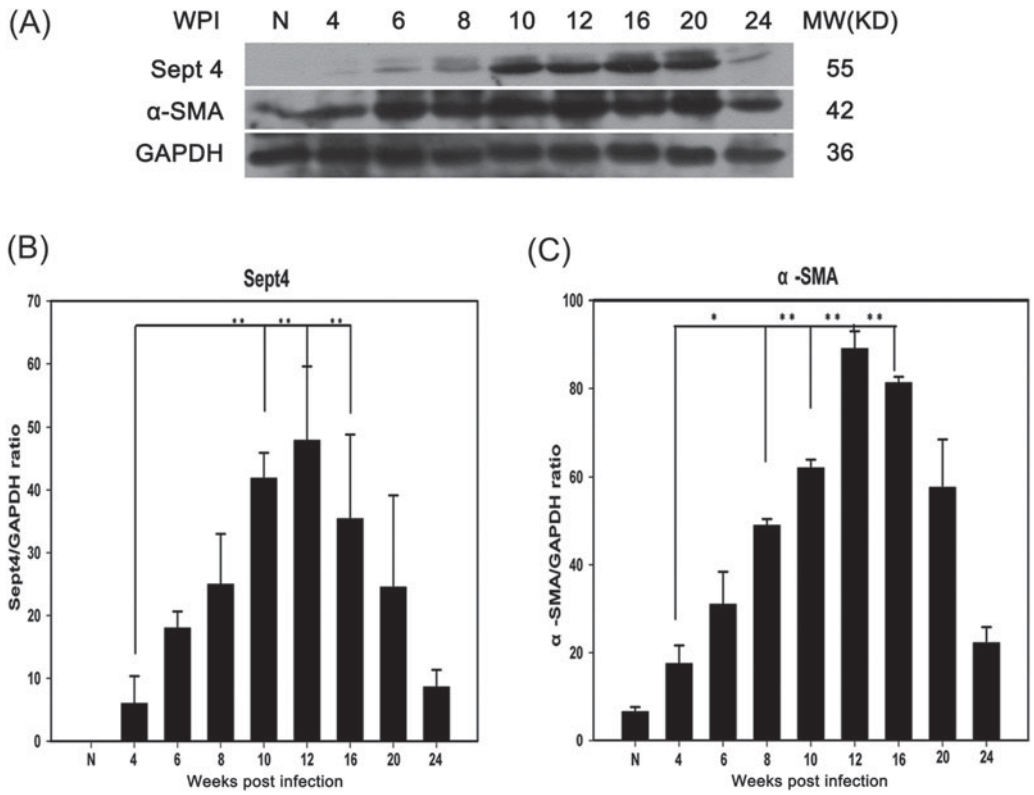

Fig. 6. Expression profile of Sept4 and α-SMA in fibrotic livers of *Schistosoma japonicum*-infected mice. (A) Western blot analyses showed that bands for Sept4 and α-SMA were at molecular weights of 55 kDa and 42 kDa, respectively. In addition, Sept4 started to appear at 4 weeks p.i., while α-SMA was present in the normal group at a low level. Both of them were increased in a time-dependent manner. (B and C) Quantitative analyses showed the ratio of Sept4 and α-SMA relative to GAPDH for each time-point. The ratios of Sept4/GAPDH and α-SMA/GAPDH were, respectively, approximately 50% and 85% at the peak at 12 weeks p.i., followed by down-regulation. The data are means ± S.E.M. (*$<0{\cdot}05$; **$p<0{\cdot}01$, *vs* 4 WPI). Experiments were repeated thrice from different mice.

demonstrating that the presence of Sept4 was low in quiescent HSCs but markedly high in culture-activated HSCs by qRT-PCR (De Minicis *et al*. 2007). However, another report has shown the opposite result on HSCs with the same method (Iwaisako *et al*. 2008). Nevertheless, these previous reports produced the same results showing that Sept4 was down-regulated in liver fibrogenesis with the model of CCl4 and BDL treatment. We hypothesized that the discrepancy may be due to the use of different models, which could differentially influence the expression of Sept4. Interestingly, we found that the expression tendencies of Sept4 and α-SMA were similar by qRT-PCR and Western blot analysis. Additionally we observed that Sept4 and α-SMA co-localized in the peri-sinusoidal space, where HSCs distribute, in the periphery of circumoval granulomas and the portal venule in *S. japonicum*-infected mice by immunofluorescence and immunohistochemistry analysis. It is known that activated HSCs express α-SMA as a cell marker and contractile machinery in various fibroses. Although accumulated studies have evaluated the importance of α-SMA as the actin isoform and other cytoskeleton filaments on HSCs function, few reports describe the role of Sept4 on HSCs. Mammalian Septins localize not only to the plasma membrane but also throughout the cytoplasm associated with the microtubule and actin cytoskeletons (Spiliotis, 2006). In various cell types, fibrillar Septin polymers co-localize with actin stress fibres through the conserved potential filament cross-linker, anillin, which can bind directly to actin through the N terminus and septin filaments by the C-terminal PH domain *in vitro* (Kinoshita *et al*. 2002). Actin depolymerization results in loss of Septin fibres, and Septin depletion in turn leads to loss of actin bundles. Reconstitution of filamentous Septin assembly requires F-actin bundles and anillin (Kinoshita *et al*. 2002). Besides these, another report showed that Septins can couple to the actin cytoskeleton through nuclear translocation of NCK by SOCS7 (Kremer *et al*. 2007). Furthermore, some studies demonstrated that α-SMA in myofibroblasts appeared to have a suppressing role in tissue fibrosis progression (Takeji *et al*. 2006) and loss of Sept4 exacerbated liver fibrosis through the dysregulation of hepatic stellate cells (Iwaisako *et al*. 2008). Based on these findings, Sept4 and α-SMA might interact together in HSCs, possibly affecting the stabilization and function of HSCs.

Furthermore, ARTS as the splice variant of Sept4 protein plays a critical role in induction and

https://doi.org/10.1017/S0031182011000667 Published online by Cambridge University Press

promotion of apoptosis. Previous reports show that ARTS/Sept4 is highly expressed in the healthy human brain but is fairly low in most of the tested schizophrenic brain samples, which indicates that ARTS may play an important role in the pathogenesis of schizophrenia (Gottfried *et al*. 2007). Whether ARTS/Sept4 in HSCs has the function of inducing apoptosis of HSCs in *S. japonicum*-induced liver fibrosis can be an interesting topic for further studies.

In conclusion, based on our observations and other previous reports, we hypothesize that Sept4 seems to be involved in the formation of inflammatory granulomata and subsequent liver fibrosis by regulating HSC activation. Additionally, given that the expression tendencies of Sept4 and α-SMA are similar, Sept4 could be a novel marker for activated HSCs *in vivo* and might be utilizable for clinical diagnosis at least in *S. japonicum* egg-induced liver fibrosis. Certainly further studies are still needed to refine the understanding of this process.

FINANCIAL SUPPORT

This work was supported by a Project funded by the Priority Academic Program Development of Jiangsu Higher Education Institutions and a grant from the Graduate Student Office of Nantong University (No. YKC09026).

REFERENCES

Arnaud, V., Li, J., Wang, Y., Fu, X., Mengzhi, S., Luo, X., Hou, X., Dessein, H., Jie, Z., Xin-Ling, Y., He, H., McManus, D. P., Li, Y. and Dessein, A. (2008). Regulatory role of interleukin-10 and interferon-gamma in severe hepatic central and peripheral fibrosis in humans infected with *Schistosoma japonicum*. *Journal of Infectious Diseases* **198**(3), 418–426. doi: 10.1086/588826.

Bartley, P., Ramm, G., Jones, M., Ruddell, R., Li, Y. and McManus, D. (2006). A contributory role for activated hepatic stellate cells in the dynamics of *Schistosoma japonicum* egg-induced fibrosis. *International Journal for Parasitology* **36**(9), 993–1001. doi: 10.1016/j.ijpara.2006.04.015.

Bataller, R. and Brenner, D. A. (2001). Hepatic stellate cells as a target for the treatment of liver fibrosis. *Seminars in Liver Disease* **21**(3), 437–451. doi: 10.1055/s-2001-17558.

Burke, M. L., Jones, M. K., Gobert, G. N., Li, Y. S., Ellis, M. K. and McManus, D. P. (2009). Immunopathogenesis of human schistosomiasis. *Parasite Immunology* **31**(4), 163–176. doi: 10.1111/j.1365-3024.2009.01098.x.

Carpino, G., Morini, S., Ginanni Corradini, S., Franchitto, A., Merli, M., Siciliano, M., Gentili, F., Onetti Muda, A., Berloco, P., Rossi, M., Attili, A. F. and Gaudio, E. (2005). Alpha-SMA expression in hepatic stellate cells and quantitative analysis of hepatic fibrosis in cirrhosis and in recurrent chronic hepatitis after liver transplantation. *Digestive and Liver Disease* **37**(5), 349–356. doi: 10.1016/j.dld.2004.11.009.

Chang, K. T., Tsai, M. J., Cheng, Y. T., Chen, J. J., Hsia, R. H., Lo, Y. S., Ma, Y. R. and Weng, C. F. (2009). Comparative atomic force and scanning electron microscopy: an investigation of structural differentiation of hepatic stellate cells. *Journal of Structural Biology* **167**(3), 200–208. doi: 10.1016/j.jsb.2009.06.005.

Chen, F., Cai, W., Chen, Z., Chen, X. and Liu, R. (2002). Dynamic changes in the collagen metabolism of liver fibrosis at the transcription level in rabbits with *Schistosomiasis japonica*. *Chinese Medical Journal* **115**(11), 1637–1640.

De Minicis, S., Seki, E., Uchinami, H., Kluwe, J., Zhang, Y., Brenner, D. A. and Schwabe, R. F. (2007). Gene expression profiles during hepatic stellate cell activation in culture and in vivo. *Gastroenterology* **132**(5), 1937–1946. doi: 10.1053/j.gastro.2007.02.033.

Field, C. M. and Kellogg, D. (1999). Septins: cytoskeletal polymers or signalling GTPases? *Trends in Cell Biology* **9**(10), 387–394. doi: 10.1016/S0962-8924(99)01632-3.

Friedman, S. L. (2000). Molecular regulation of hepatic fibrosis, an integrated cellular response to tissue injury. *The Journal of Biological Chemistry* **275**(4), 2247–2250. doi: 10.1074/jbc.275.4.2247.

Friedman, S. L. (2003). Liver fibrosis – from bench to bedside. *Journal of Hepatology* **38** (Suppl 1), S38–S53. doi: 10.1016/S0168-8278(02)00429-4.

Friedman, S. L. (2008). Hepatic fibrosis – overview. *Toxicology* **254**(3), 120–129. doi: 10.1016/j.tox.2008.06.013.

Gottfried, Y., Rotem, A., Klein, E. and Larisch, S. (2007). The pro-apoptotic ARTS/Sept4 protein is significantly reduced in post-mortem brains from schizophrenic patients. *Schizophrenia Research* **96**(1–3), 257–266. doi: 10.1016/j.schres.2007.05.031.

Ihara, M., Kinoshita, A., Yamada, S., Tanaka, H., Tanigaki, A., Kitano, A., Goto, M., Okubo, K., Nishiyama, H. and Ogawa, O. (2005). Cortical organization by the septin cytoskeleton Is essential for structural and mechanical integrity of mammalian spermatozoa. *Developmental Cell* **8**(3), 343–352. doi: 10.1016/j.devcel.2004.12.005.

Iwaisako, K., Hatano, E., Taura, K., Nakajima, A., Tada, M., Seo, S., Tamaki, N., Sato, F., Ikai, I., Uemoto, S. and Kinoshita, M. (2008). Loss of Sept4 exacerbates liver fibrosis through the dysregulation of hepatic stellate cells. *Journal of Hepatology* **49**(5), 768–778. doi: 10.1016/j.jhep.2008.05.026.

Kinoshita, A., Noda, M. and Kinoshita, M. (2000). Differential localization of septins in the mouse brain. *The Journal of Comparative Neurology* **428**(2), 223–239. doi: 10.1002/1096-9861(20001211)428:2<223::AID-CNE3>3.0.CO;2-M.

Kinoshita, M. (2006). Diversity of septin scaffolds. *Current Opinion in Cell Biology* **18**(1), 54–60. doi: 10.1016/j.ceb.2005.12.005.

Kinoshita, M., Field, C. M., Coughlin, M. L., Straight, A. F. and Mitchison, T. J. (2002). Self- and actin-templated assembly of mammalian septins. *Developmental Cell* **3**(6), 791–802. doi: 10.1016/S1534-5807(02)00366-0.

Kissel, H., Georgescu, M. M., Larisch, S., Manova, K., Hunnicutt, G. R. and Steller, H. (2005). The Sept4 septin locus is required for sperm terminal differentiation in mice. *Developmental Cell* **8**(3) 353–364. doi: 10.1016/j.devcel.2005.01.021.

Kremer, B. E., Adang, L. A. and Macara, I. G. (2007). Septins regulate actin organization and cell-cycle arrest through nuclear accumulation of NCK mediated by SOCS7. *Cell* **130**(5), 837–850. doi: 10.1016/j.cell.2007.06.053.

Lindert, S., Wickert, L., Sawitza, I., Wiercinska, E., Gressner, A. M., Dooley, S. and Breitkopf, K. (2005). Transdifferentiation-dependent expression of alpha-SMA in hepatic stellate cells does not involve TGF-beta pathways leading to coinduction of collagen type I and thrombospondin-2. *Matrix Biology* **24**(3), 198–207. doi: 10.1016/j.matbio.2005.03.003.

Spiliotis, E. T. (2006). Here come the septins: novel polymers that coordinate intracellular functions and organization. *Journal of Cell Science* **119**(1), 4–10. doi: 10.1242/jcs.02746.

Takeji, M., Moriyama, T., Oseto, S., Kawada, N., Hori, M., Imai, E. and Miwa, T. (2006). Smooth muscle alpha-actin deficiency in myofibroblasts leads to enhanced renal tissue fibrosis. *The Journal of Biological Chemistry* **281**(52), 40193–40200. doi: 10.1074/jbc.M602182200.

Wilson, M. S., Mentink-Kane, M. M., Pesce, J. T., Ramalingam, T. R., Thompson, R. and Wynn, T. A. (2007). Immunopathology of schistosomiasis. *Immunology and Cell Biology* **85**(2), 148–154. doi: 10.1038/sj.icb.7100014.

Wynn, T. A., Thompson, R. W., Cheever, A. W. and Mentink-Kane, M. M. (2004). Immunopathogenesis of schistosomiasis. *Immunological Reviews* **201**, 156–167. doi: 10.1111/j.0105-2896.2004.00176.x.

Zhang, L. H., Pan, J. P., Yao, H. P., Sun, W. J., Xia, D. J., Wang, Q. Q., He, L., Wang, J. and Cao, X. (2001). Intrasplenic transplantation of IL-18 gene-modified hepatocytes: an effective approach to reverse hepatic fibrosis in schistosomiasis through induction of dominant Th1 response. *Gene Therapy* **8**(17), 1333–1342. doi: 10.1038/sj.gt.3301524.

Zieger, B., Tran, H., Hainmann, I., Wunderle, D., Zgaga-Griesz, A., Blaser, S. and Ware, J. (2000). Characterization and expression analysis of two human septin genes, PNUTL1 and PNUTL2. *Gene* **261**(2), 197–203. doi: 10.1016/S0378-1119(00)00527-8.